PHILOSOPHICAL TRANSACTIONS OF THE ROYAL SOCIETY A
MATHEMATICAL, PHYSICAL & ENGINEERING SCIENCES

The first galaxies: structure and stellar populations

Mark Dickinson

Phil. Trans. R. Soc. Lond. A 2000 **358**, 2001-2019
doi: 10.1098/rsta.2000.0626

10.1098/rsta.2000.0626

The first galaxies: structure and stellar populations

By Mark Dickinson

Space Telescope Science Institute, 3700 San Martin Drive, Baltimore, MD 21218, USA

The Hubble deep fields (HDFs) continue to be a valuable resource for studying the distant Universe, particularly at $z > 2$ where their comoving volume becomes large enough to encompass several hundred L^* galaxies or their progenitors. Here, I present recent results from a near-infrared (NIR) imaging survey of the HDF-north with the Near Infrared Camera and Multi-Object Spectrograph (NICMOS), which provides structural and photometric information in the optical rest frame ($\lambda\lambda_0$4000–5500 Å) for hundreds of 'ordinary' galaxies at $2 < z < 3$, and which offers the means to search for still-more-distant objects at $z \gg 5$. Lyman-break galaxies (LBGs) at $2 < z < 3$ are compact and often irregular in the NICMOS images; ordinary Hubble sequence spirals and ellipticals seem to be largely absent at these redshifts, and apparently reached maturity at $1 < z < 2$. The LBGs have ultraviolet (UV)–optical spectral energy distributions like those of local starburst galaxies. Population synthesis models suggest typical ages of a few $\times\, 10^8$ years and moderate UV extinction (*ca.* 1.2 mag at 1700 Å), but the constraints are fairly weak and there may be considerable variety. Considering an NIR selected galaxy sample, there is little evidence for a significant number of galaxies at $z \sim 3$ that have been missed by UV-based Lyman-break selection. Using the well-characterized $z \sim 3$ galaxy population as a point of reference, I consider LBG candidates at $4.5 < z < 9$, as well as one remarkable object that might (or might not) be an LBG at $z > 12$. The space density of UV-bright galaxies in the HDF appears to thin out toward larger redshifts, although surface-brightness selection effects may play an important role.

Keywords: early Universe; evolution; morphology; stellar content; galaxies

1. Introduction

(a) *The first galaxies?*

The past five years have seen remarkable breakthroughs in our ability to identify and systematically study ordinary galaxies at very large redshifts, not just as isolated case studies, but *en masse* as a galaxy *population*. To date, nearly 1000 galaxies have been spectroscopically confirmed at $z > 2$, mostly identified via broadband colour-selection techniques (see Steidel *et al.* (1996), i.e. the Lyman-break galaxies (LBGs)), but with other important and complementary methods also coming into play (submillimetre (SMM)) and radio surveys, emission line searches, quasi-stellar object (QSO) absorption systems, etc.). A broad census of galaxy properties at $z \sim 3$

now seems within reach, covering star-formation rates (SFRs), dust content, morphologies, spatial clustering, and perhaps even chemical abundances and internal kinematics.

Although I have retained my assigned title, 'The first galaxies...', it is far from clear that we know when, where or how to find the 'first' galaxies. The $z \sim 3$ LBGs may or may not be the first major wave of galaxy formation. If anything, current data favour a roughly constant global SFR (as traced by cosmic ultraviolet (UV) luminosity density, at least) from $2 \lesssim z \lesssim 4$, with no certain evidence for a decline at higher redshifts (Steidel *et al.* 1999). The SMM population detected by the Submillimetre Common User Bolometer Array (SCUBA) (cf. Cowie, this issue) may or may not represent the bulk of early star formation, and the upper redshift bound to SCUBA sources remains unknown. The reionization of the intergalactic medium at $z > 5$ and the presence of metals in the Lyα forest at $z \sim 3$ point toward earlier epochs of star and galaxy formation, at least in trace amounts. A handful of galaxies now have plausible spectroscopic confirmation at $z > 5$, but too few for any systematic census.

For this reason, I cannot promise to live up to my title: I do not know what the first galaxies are or what they look like. Given this ignorance, in the first part of this article I will focus on the structure and stellar populations of the most-distant *well-studied* galaxies, the $z \sim 3$ Lyman-break objects. This is not meant as a comprehensive review, but will instead concentrate on new imaging and photometric data from the Near Infrared Camera and Multi-Object Spectrograph (NICMOS) on-board the Hubble Space Telescope (HST) that extend our knowledge of LBG properties to the optical rest frame. In his contribution to this issue, Max Pettini provides a complementary discussion of recent efforts to measure chemical abundances and internal kinematics for these same galaxies. In the second part of my article, I will describe efforts to extend Lyman-break colour selection to still larger redshifts, approaching (or perhaps even exceeding) $z \approx 10$. In this way I hope to at least provide a look into the epoch when 'the first galaxies' might plausibly have been formed, and to catalogue what we can find right now, in the pre-Next Generation Space Telescope (pre-NGST) era, given the best available survey data.

(*b*) *Infrared observations of the Hubble deep field*

For the past five years, the Hubble deep fields (HDFs) have provided the most exquisitely deep, high-angular-resolution optical census of the distant Universe. It is important (if somewhat pedantic) to consider what an HDF is actually good for. One WFPC2 field covers 5 arcmin^2, and probes a very small comoving volume at $z < 1$, enough to hold only *ca.* 12–30L^* galaxies, depending on the cosmology. Given small-number statistics and concerns about clustering, the central HDF is, therefore, not the best place to study massive galaxies in the 'low'-redshift Universe, despite the fact that most of cosmic time and most bright galaxies with spectroscopic redshifts are at $z \lesssim 1$. There is far more volume at high redshift: 10.5–40 times more at $2 < z < 10$ than at $z < 1$ for plausible cosmologies, room enough for several hundred L^* galaxies or their progenitors.

At $z > 1$, the optical light emitted from galaxies shifts into the near infrared (NIR). Thus, in order to compare $z > 2$ galaxies with their local counterparts, and to search for still-more-distant objects at $z \gg 5$, it is important to extend the wavelength baseline. The HDF-north was observed in the NIR from the ground in several different programmes (see, for example, Hogg *et al.* (1997), Barger *et al.* (1999), and our own Kitt Peak National Observatory (KPNO) 4m J, H and K_s (JHK_s) filter imaging; cf. Dickinson (1998)). The depth and angular resolution (typically *ca.* 1 arcsec) of these data are a poor match to those of the optical WFPC2 HDF images. Two programmes therefore targeted the HDF-north with the NICMOS on board the HST, providing much deeper images with high angular resolution. The NICMOS guaranteed time observers (GTOs) (Thompson *et al.* 1999) imaged one NICMOS camera 3 field (*ca.* 51×51 arcsec^2) for 49 orbits each at F110W (1.1 μm) and F160W (1.6 μm). Our own programme mosaicked the complete HDF with a mean exposure time of 12 600 s per filter in F110W and F160W. Sensitivity varies over the field of view, but the average depth is AB $\approx$ 26.1 at $S/N = 10$ in an $0''.7$ diameter aperture. The drizzled point spread function (PSF) has a full-width half-maximum (FWHM) of $0''.22$, primarily limited by the NIC3 pixel scale. Because most galaxies have spectral energy distributions (SEDs) that brighten (in f_ν units) at redder wavelengths, our images detect roughly half of the galaxies from the WFPC2 HDF, despite their short exposure times. We have also re-analysed our KPNO K_s images to optimally extract photometry matched to the WFPC2 + NICMOS data. These data are not as deep as one would like, which is unfortunate because they provide the only access to rest-frame optical wavelengths for objects at $3 < z < 4.4$, but they are the best presently available.

Thanks to the dedicated efforts of the observers, a remarkably high density of spectroscopic redshifts is available in the HDF-north: approximately 150 galaxies (plus a few stars) in the central WFPC2 + NICMOS field alone, with 33 objects at $2 < z < 5.6$. Taking advantage of the high-quality photometric data, many investigators have used multicolour selection (e.g. the two-colour Lyman-break criteria of Steidel *et al.* (1996), Madau *et al.* (1996), and others) or photometric redshifts (see, for example, Fernández-Soto *et al.* 1999) to identify high-redshift-galaxy candidates. There are advantages and drawbacks to both approaches, but both have demonstrated remarkable successes. In this discussion, I will make use of both methods. For the photometric redshifts, I will use fits to our seven-band HDF photometry by Budavári *et al.* (2000), whose 'adaptive template' method is a modification of an otherwise straightforward spectral template-fitting scheme. I will use AB magnitudes here throughout, and notate the six WFPC2 + NICMOS bandpasses by U_{300}, B_{450}, V_{606}, I_{814}, J_{110} and H_{160}. Unless stated otherwise, I will assume a cosmology with $\Omega_M = 0.3$, $\Omega_\Lambda = 0.7$, and $H_0 = 70$ km s^{-1} Mpc^{-1}.

2. Galaxy morphologies at $2 < z < 3$

The NICMOS H_{160} images sample rest-frame wavelengths in the optical V- to B-bands from $z = 2$ to 2.8. This upper bound is about the midpoint of the redshift range, where 'U_{300}-dropout' Lyman-break selection in the HDF is most efficient. Therefore, at these redshifts we may use the NICMOS data to study the morphologies of LBGs at wavelengths where long-lived stars, if they are present, may dominate the light from the galaxy, and where dust obscuration should play a significantly lesser role than it does in the UV. For LBGs at $z \gtrsim 3$, the NICMOS H_{160} bandpass slips into the rest-frame UV, and the NICMOS images once again tell us more about the distribution of star formation within galaxies than about that of their stellar mass.

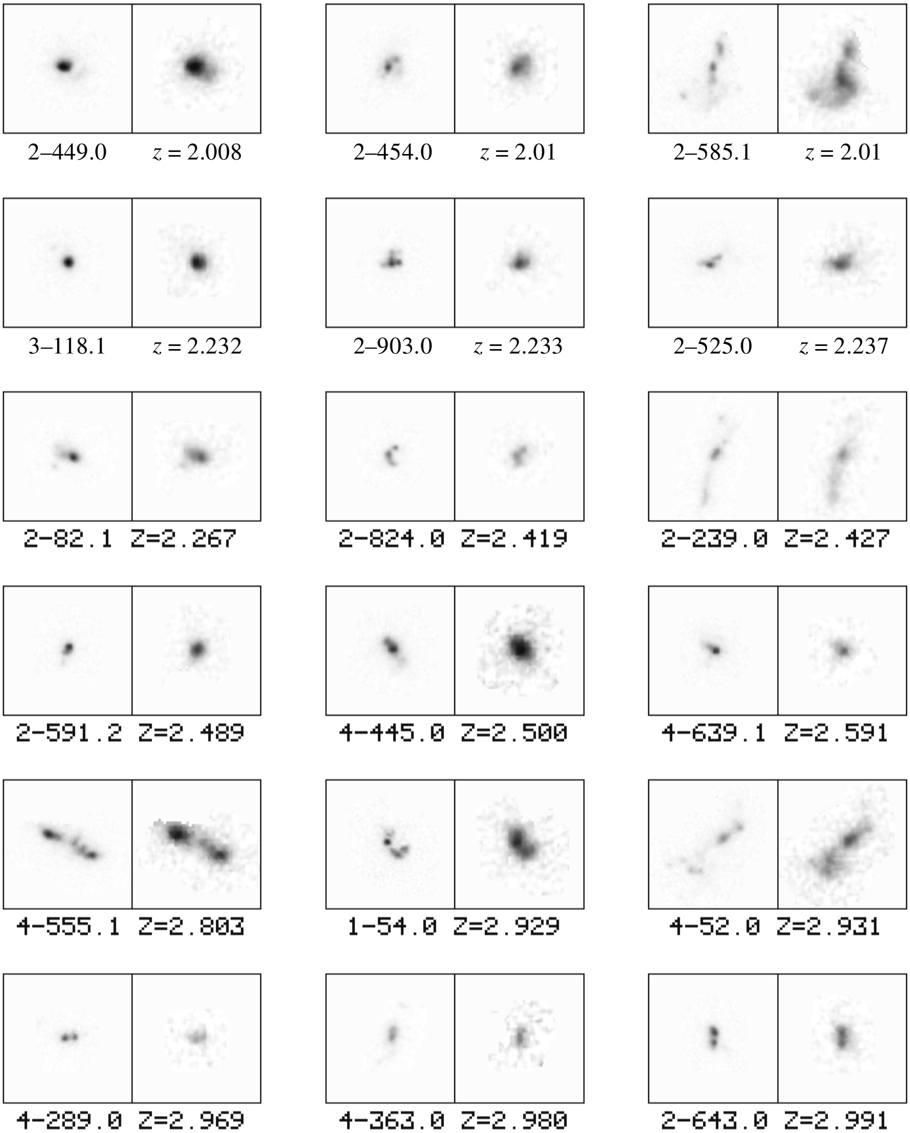

Figure 1. UV and optical rest-frame images of HDF LBGs with spectroscopic redshifts $2 < z < 3$. For each object, the left-hand image is interpolated between WFPC2 passbands to λ_0 1700 Å, while the right-hand panel interpolates the NICMOS images to the rest frame B-band (4300 Å). Galaxies at $2.8 < z < 3$ use the NICMOS H_{160} images without extrapolation. Boxes are 4×4 arcsec^2, or $32h_{70}^{-1}$ kpc on a side at $z = 2.5$. Here, the WFPC2 images have *not* been convolved to match the NICMOS PSF.

Figure 1 compares rest frame UV and optical images of a set of HDF LBGs with spectroscopic redshifts $2 < z < 3$. The NICMOS data have somewhat poorer angular resolution (0″.22 compared with 0″.14 for WFPC2), but otherwise the most striking thing is the broad similarity of the UV and optical morphologies. Giavalisco *et al.* (1996) and Lowenthal *et al.* (1997) have emphasized the very small sizes of LBGs in WFPC2 images, and the same is true at the NICMOS wavelengths. Accounting for PSF differences, the half-light radii of the galaxies measured from the NICMOS images are the same as (or in some cases, slightly smaller than) those from the WFPC2 data. Notable morphological differences are seen in only a few cases, e.g. 2–585.1 ($z = 2.008$) and 4–52 ($z = 2.931$), two of the largest LBGs in the HDF. Each has a region of diffuse emission in the WFPC2 images that 'lights up' in the NICMOS H_{160} data, with quite red colours. It is not clear whether this is due to the presence of dust, older and redder starlight, or possibly strong line emission.†

Generally, there is no evidence that the UV-bright regions seen by WFPC2 are just star-forming 'fragments' embedded within some larger, mature host galaxy. On the whole, one or more of the following appears to be true.

(1) Stars that dominate the light at $\lambda\lambda_0$1200–1800 Å also dominate at $\lambda\lambda_0$4000–5500 Å.

(2) If components with substantially different ages and colours are present, then they are fairly well mixed, spatially.

(3) Dust extinction does not play a dominant role in shaping the morphologies of LBGs at these wavelengths.

All of this should be taken *modulo* the important caveat that at FWHM = $0''.22$ resolution, most of the LBGs are *not* exquisitely resolved: they are typically very small, having only a few resolution elements within their isophotally detectable areas, and, thus, many details are surely lost except perhaps for the few, largest objects.

It is striking that among the NICMOS images of approximately 100 HDF LBGs (those with and without spectroscopic redshifts), virtually *none* resembles a 'classical' Hubble sequence spiral galaxy. Giant disc galaxies are found in the HDF and elsewhere out to at least $z \approx 1.3$ (see examples from the NICMOS in, for example, Bunker (1999) and Dickinson (2000)), and various studies have found that their structural properties and comoving abundances have not changed dramatically since $z \approx 1$ (Lilly *et al*. 1998; Simard *et al*. 1999). At $z > 2$, however, there appear to be no objects with immediately recognizable spiral structure, no bulges surrounded by symmetric, diffuse discs, nor even good candidates for thin, edge-on discs (some LBGs are fairly elongated, but none could really be mistaken for an edge-on spiral). Among the objects shown in figure 1, perhaps 2–585.1 ($z = 2.008$) appears closest to showing spiral structure at rest-frame optical wavelengths, but this requires some imagination. Given the evidence from the NICMOS, the absence of classical spiral morphologies cannot be attributed solely to rest-frame wavelength effects. We have carried out simulations using optical rest-frame images of Virgo cluster spirals and of HDF disc galaxies at $z < 1$, artificially inserted into the NICMOS images at high redshift with the appropriate surface-brightness dimming and PSF convolution. Although low surface brightnesses and limited angular resolution wipe out many of the details of spiral structure, giant ($L > L^*$) disc galaxies should be detectable and recognizable at $z > 2$ even with *no* luminosity or surface-brightness evolution. This is not to say that LBGs cannot be disc galaxies: as already noted, the small angular sizes of most LBGs preclude detailed resolution, and some of these objects could well

† 4–52 is one of the few $z > 2$ galaxies detected at 8.5 GHz by Richards *et al*. (1998). The radio centroid is coincident with the diffuse, red, IR-bright region in the galaxy.

be small discs. Indeed, Giavalisco *et al*. (1996) noted exponential surface-brightness profiles among some LBGs.

Giavalisco *et al*. (1996) also found that some LBGs have $R^{1/4}$-law profiles, although it is not clear whether to interpret this as indicating a relation between LBGs and present-day ellipticals and bulges. It is worth noting, however, that there are few candidates for intrinsically *red* elliptical galaxies at $z > 2$ in the HDF, i.e. objects that would be recognized as elliptical galaxies today both by morphology and by the characteristic colour signature of an older stellar population. In fact, considering objects with spectroscopic or photometric redshifts in the range $2 < z < 4$, where the NICMOS+KPNO IR data still reach the optical rest frame, there are only a handful of galaxies with rest-frame colours redder than that of a present-day Scd spiral (i.e. an actively star-forming galaxy), even in an IR-selected sample, which should have no bias against such objects. I return to this point in § 4 below. Nearly every HDF galaxy at $z > 2$ that is detectable at 1.6 μm appears to be forming stars, and most quite vigorously. We *do* find apparently red, dead ellipticals in the HDF out to (photometric) redshifts of $z \approx 1.8$ (cf. Dickinson 2000; Stanford *et al*. 2000), but only one (marginally) viable candidate for a red elliptical at higher redshift. This is the so-called '*J*-dropout' object HDFN-JD1 (see § 6), whose colours might be matched by those of a maximally old elliptical galaxy at $3 < z < 4$ (Dickinson *et al*. 2000).†

Overall, it seems that the maturation of the giant spiral and elliptical galaxies took place at $z < 2$. Even with extremely deep, high-angular-resolution IR images like the HDF/NICMOS data, we find few (if any) mature spirals or ellipticals (or candidates for such) at higher redshift. By $z = 1$, many (if not necessarily all) large spirals and red giant ellipticals were already in place, pointing to the redshift range $1 < z < 2$ as an important 'golden age' for the formation of the Hubble sequence.

3. Galaxy colours at $2 < z < 3.5$

Figure 2 shows a photometric compendium of spectroscopically confirmed HDF galaxies at $2 < z < 3.5$, all shifted to the rest frame and normalized to a common flux density at $\lambda_0 2000$ Å. The shaded envelope is defined by local UV-to-optical starburst galaxy spectral templates from Kinney *et al*. (1996), which span a broad range in optical–UV extinction. The HDF LBGs fall comfortably within the range of SED shapes defined by the local starbursts. They have relatively blue (but usually not flat spectrum) UV continua, with a flux increase and spectral inflection around the Balmer/4000 Å break region that indicates the presence of older (A and later) stars, which apparently contribute a significant fraction of the rest-frame optical light. The fact that the UV continuum slope for LBGs is nearly always redder than flat spectrum has generally been interpreted as an indication of dust extinction (see, for example, Meurer *et al*. 1997, 1999; Dickinson 1998; Pettini *et al*. 1998), although for some objects it might also result from an ageing stellar population with declining or inactive star formation. Considered individually, the large majority of HDF LBGs are reasonably well fit by the Kinney *et al*. (1996) starbursts with modest reddening ($0 < E(B - V) < 0.21$). Few approach the more-heavily reddened templates. This may be true by definition/selection, of course, since we are considering the brighter

† In fact, HDFN-JD1 is probably too red for an old stellar population at high redshift without invoking dust, an unusual initial mass function (IMF), or an unfashionable cosmological model.

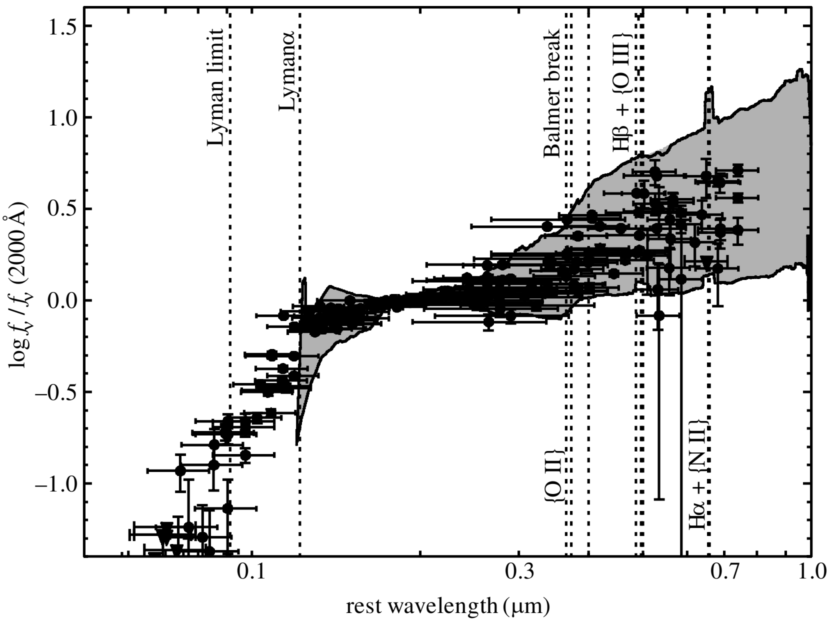

Figure 2. Photometry for 27 HDF galaxies with spectroscopic redshifts $2 < z < 3.5$, shifted to the rest frame and normalized at 2000 Å. The shaded region spans the range of empirical starburst templates from Kinney *et al.* (1996). The starburst SED sequence is primarily defined by reddening up to $E(B-V) \lesssim 0.7$; the blue envelope is set by NGC 1705.

objects for which redshifts were successfully measured, and which were selected for spectroscopy by their UV colours (but see § 4 below).

With photometry spanning the UV-to-optical rest frame it becomes interesting to compare the LBG photometry with population synthesis models to look for constraints on galaxy ages, reddening, and star formation histories. Very roughly, if the UV spectral slope provides a measure of extinction (modulo an assumed reddening law), then the UV–optical flux ratio, and, particularly, the amplitude of any inflection around the Balmer/4000 Å break region, may help constrain the past star-formation history, particularly the ratio of older stars to ongoing star formation. This was first done by Sawicki & Yee (1998) using ground-based JHK_s photometry for LBGs in the HDF. Their results favoured young ages (median value *ca.* 25 Myr) and fairly heavy reddening (typical $E(B-V) \approx 0.28$, or 3 mag extinction at 1600 Å assuming Calzetti (1997) starburst dust attenuation). We have carried out a similar exercise using the NICMOS data and K-band fluxes rederived from the KPNO data using a technique (much like that of Fernández-Soto *et al.* (1999)) that properly matches photometry from images with very different angular resolutions. A complete presentation will be given in Papovich *et al.* (2000) and is beyond the scope of the present discussion, but I summarize some important points here.

Even with precise NICMOS photometry, constraints on ages and reddening are quite loose. This is, in part, because of the usual degeneracies in fitting models to broadband colours (age versus metallicity versus extinction), but also because the available photometry simply does not reach long-enough rest-frame wavelengths. At $z > 3$, only the lower-S/N ground-based K_s data extend redward of the Balmer/

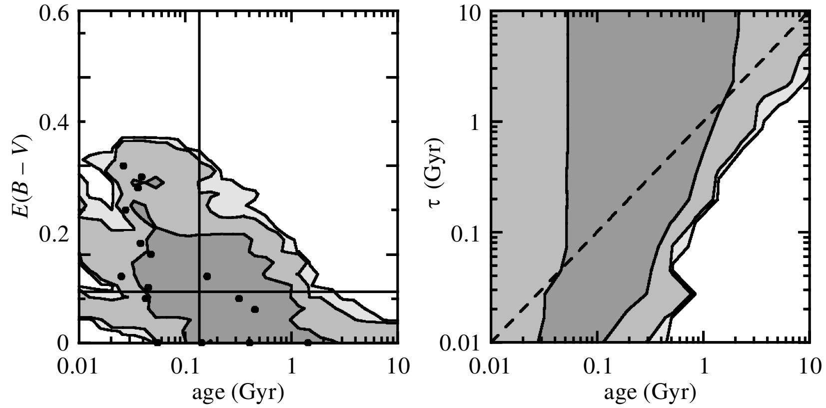

Figure 3. Combined confidence intervals (68%, 95%, 99.7%) for population synthesis model fits to a sample of 16 HDF LBGs with spectroscopic redshifts $2 < z < 2.95$ (from Papovich *et al.* (2000)). A wide range of G. Bruzual & S. Charlot (1996, personal communication) models has been considered with varying age (t), star-formation histories (exponential time-scale τ), dust attenuation ($E(B-V)$, here assuming the Calzetti (1997) starburst law), metallicity, and IMF. Here, results for the 16 objects have been averaged—weighted by their individual probability distributions—to show the ensemble likelihood distributions for $E(B-V)$, t and τ. Best-fitting values for each object are marked by points in part (a). Dependences on metallicity and IMF have been collapsed, but are fairly weak. The cross-hairs in (a) indicate the most-favoured values for $E(B-V)$ versus t. The dashed line in (b) marks $t = \tau$. Models observed after the bulk of their star formation has been completed (i.e. $t \gg \tau$) are disfavoured, except at young ages ($\lesssim$ a few $\times 10^8$ yr) and short time-scales, when the UV continuum can persist throughout the main sequence lifetimes of B stars.

4000 Å break region; for this reason, I only consider galaxies at $2 < z < 3$ here. For each galaxy, we may define confidence intervals in the multidimensional space of the various fitting parameters such as age, SFR e-folding time-scale, reddening, metallicity and IMF. The colour degeneracies allow fairly broad ranges in acceptable parameters for each object, and the variety among the galaxy SEDs (figure 2) scatters the best-fitting parameters throughout a range of values. Nevertheless, taken as an ensemble, certain regions of model parameter space are preferred.

Figure 3 shows a composite distribution for 16 galaxies with $z < 3$, where model fits for each object have been averaged, weighted by their likelihoods in the multi-parameter space. The contours thus indicate a distribution of likely parameter values for the ensemble of UV-selected LBGs. The best-fitting values of $E(B-V)$ versus age for individual objects are marked by dots. Some galaxies can be fit reasonably well by parameter values falling toward the outer contours of the ensemble distribution, but the majority occupy the higher confidence regions. The most-favoured age range spans 0.03–1 Gyr, with extinction $0 < E(B-V) < 0.25$. The extinction values agree well with the comparison with the Kinney *et al.* (1996) starburst templates (figure 2), which is not unexpected given that the Calzetti attenuation law is derived in part from the same UV spectral data on local starburst galaxies. The range of likely age and extinction values becomes slightly smaller and can shift somewhat if restrictions on metallicity or IMF are adopted, although, in general, the broadband photometry offers little constraint on these parameters. Younger ages and larger extinctions are allowed and even favoured for some objects, but, in general, the most likely values are somewhat older and less reddened than those found by Sawicki & Yee (1998). This may be due to more-precise photometry from the NICMOS, or to better control of the relative optical–IR colours (particularly in the K-band) from our photometric method.

It is not clear whether the apparent anticorrelation between age and extinction in figure 3 is significant. We expect degeneracy between the age and extinction values fit to individual objects, but the overall trend seen in the population may be greater than would be expected from the fitting uncertainties alone. The 'most-favoured' extinction value, $E(B-V) \approx 0.12$, corresponds to $A(1700\ \text{Å}) \approx 1.2$ mag, or a factor of approximately 3. The *net* UV extinction for the sample (and, hence, the correction to any derived global star-formation rate) would be larger, however, driven by the objects with the greatest reddening.

A characteristic time-scale for LBGs can be defined from their sizes (median half-light radii of *ca.* 2.2 kpc for the HDF LBGs) and typical velocity dispersions (*ca.* 80 km s^{-1}; see Pettini, this issue). This yields $t_c \sim 25$ Myr. If the UV light is due to ongoing star formation, we would not expect SFR lifetimes $\ll t_c$, and, indeed, this is roughly the lower bound of the best-fit model age range, with the 'most-favoured' value being *ca.* 135 Myr, or approximately $5t_c$. This range is not dissimilar to that estimated for star formation in galactic-scale starburst events (e.g. ultraluminous infrared galaxies) locally.

4. Rest-frame UV selection: what do we miss?

Using an IR-selected catalogue, we may ask what galaxies might be missed altogether by Lyman-break colour selection keyed to the rest-frame UV light. In particular, one might expect some red high-redshift galaxies, either because they are not actively forming stars or because of extinction, that would 'drop out' of the dropout samples. Here, I restrict my analysis to $H_{160} < 26$, where we believe our catalogues are highly complete, uncontaminated by spurious sources, and where the NICMOS photometry has $S/N \gtrsim 10$. At $z = 2.75$, $H_{160} < 26$ corresponds to rest frame $M_B < -19.36$ for the adopted cosmology, or *ca.* 1 mag fainter than present-day L_B^*. The typical LBG at $H_{160} \approx 26$ has $V_{606} \approx 27$, the practical limit for HDF U_{300}-dropout selection using standard two-colour criteria, but red galaxies with similar rest-frame optical luminosities might be fainter or absent in the UV.

At $H_{160} < 26$ there is only one object that is undetected with $S/N < 2$ in V_{606} or I_{814} (both, in this case): this is the 'J-dropout' HDFN-JD1 (see also §§2 and 6). In fact, this is the only NICMOS-selected object with $H_{160} < 26$ and $S/N(I_{814}) < 6.5$. Two other objects have $S/N(V_{606}) < 3$; both are $z \gtrsim 5$ 'V_{606}-dropout' candidates identified by Lanzetta *et al.* (1996) and Fernández-Soto *et al.* (1999), one of which (3–951) was spectroscopically confirmed at $z = 5.33$ (Spinrad *et al.* 1998). Thus, the only possible candidate for a NICMOS-selected, 'UV-invisible' galaxy at $z \sim 3$ is HDFN-JD1.

Next let us consider UV-bright objects that might, nevertheless, have been missed by the LBG colour criteria, using the seven-band photometric redshift estimates for all galaxies. In principle, these may identify plausible candidates at $2 < z < 3.5$ that otherwise fall outside a given set of UV colour criteria, as long as their intrinsic SEDs are 'recognizably similar' to those of galaxies at lower redshift, which define the templates used for the photometric redshift fitting.

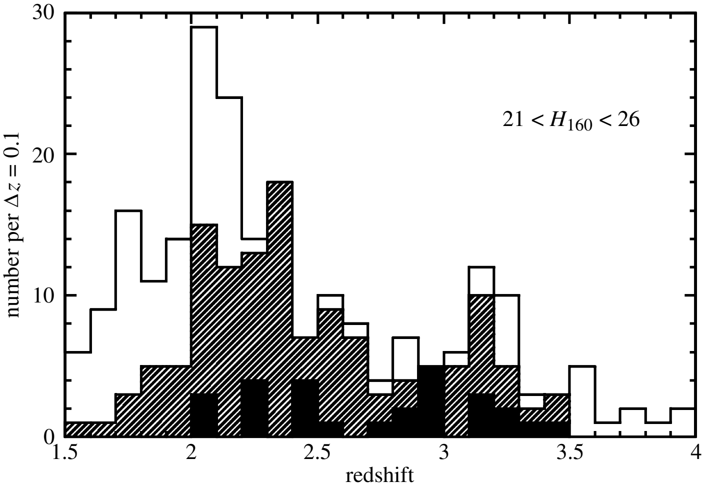

Figure 4. Photometric and spectroscopic redshift distributions for IR-selected HDF galaxies ($H_{160} < 26$) at $1.5 < z < 4$. The open histogram shows the $z_{\rm phot}$ distribution from Budavári *et al*. (2000). The hatched histogram indicates galaxies that obey the Lyman-break criteria defined in the text, while the filled histogram shows the available spectroscopic redshifts.

Figure 4 shows the $z_{\rm phot}$ distributions for all HDF galaxies with $21 < H_{160} < 26$, and for those that meet the U_{300} 'dropout' criteria $(U_{300} - B_{450}) > (B_{450} - V_{606}) + 1$ and $B_{450} - V_{606} < 1.2$ from Dickinson (1998). There are 43 objects with $2 < z_{\rm phot} < 3.5$ which do *not* meet the LBG colour criteria. However, nearly all are at $2 < z_{\rm phot} < 2.2$ or $3.2 < z_{\rm phot} < 3.5$, and lie just outside the colour-selection boundaries defined here: either slightly too blue at low z, or slightly too red at high z. This is expected: the selection efficiency of the two-colour method is not uniform with redshift, and falls off at the extremes of the range for which it is optimized (cf. Steidel *et al*. 1999). Only seven 'missed' objects fall at intermediate photometric redshifts, $2.5 < z_{\rm phot} < 3.1$, and most of these are also just outside the colour-selection box. Some are quite interesting, including a μJy radio source with very red $J_{110} - H_{160}$ colours, which may be a dusty starburst or a fading post-starburst galaxy at $z \sim 2.6$. Others may be scattered out of the box by photometry errors (especially in U_{300}), or might not be at the indicated $z_{\rm phot}$. But all are well detected in the optical HDF.

Overall, there is no evidence for a *substantial* population (by number) of galaxies at $2 < z < 3.5$ that are missed by UV Lyman-break colour selection but that are detectable in the NIR. If there are energetically important but highly obscured galaxies at these redshifts, like those detected by SCUBA, then they are either *also* detectable with optical imaging data, or they are so heavily enshrouded that even the NICMOS cannot easily see them. For the five SMM sources detected in the HDF by Hughes *et al*. (1998), our NICMOS images do not reveal any new counterparts previously undetected by WFPC2, nor do any of the candidate identifications have particularly unusual optical–IR colours.

5. Galaxies at $4.5 \lesssim z \lesssim 9$

The successes of colour-selection techniques at $2 \lesssim z \lesssim 4.5$ make it tempting to extend the methods to higher redshifts, i.e. to search for V- or I-dropouts. Doing

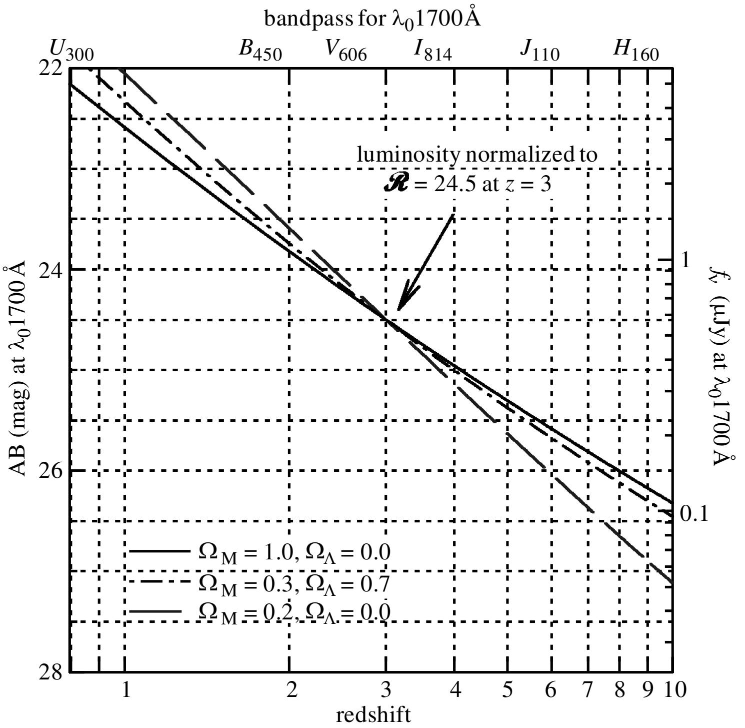

Figure 5. Apparent magnitude for an L^* ($\lambda_0$1700 Å at $z \approx 3$; see Steidel *et al.* (1999)) LBG redshifted without evolution. No k-correction is included: instead, the detection bandpass is taken to be fixed to $\lambda_0$1700 Å and changes with redshift (see top axis labels). An L^* LBG should be detectable in the NICMOS data ($H_{160} < 26.5$) out to $z \approx 10$ for spatially flat cosmologies with $\Lambda < 0.8$, and to $z \approx 7.5$ for an open universe.

PHILOSOPHICAL TRANSACTIONS OF THE ROYAL SOCIETY A MATHEMATICAL, PHYSICAL & ENGINEERING SCIENCES

so properly requires deep NIR data to provide at least one colour longward of the redshifted 912 Å and 1216 Å breaks. Indeed, galaxies at $z > 6.5$ should have virtually no detectable optical flux. Lanzetta *et al.* (1996) and Fernández-Soto *et al.* (1999) identified candidate $z \gtrsim 5$ HDF galaxies from $V_{606} - I_{814}$ colours supplemented by IR limits from the KPNO data; two of these have subsequently been confirmed via spectroscopy (Weymann *et al.* 1998; Spinrad *et al.* 1998). With the NICMOS we can extend this to fainter limits and larger redshifts: an L^* LBG (i.e. L^* in the rest frame UV at $z = 3$) should be detectable in the NICMOS images with $H_{160} < 26.5$ out to $z = 10$ for spatially flat cosmologies with $\Lambda \leqslant 0.8$, and out to $z \approx 7.5$ for an $\Omega_M = 0.2$ open universe (see figure 5).

Here we test the null hypothesis that the galaxy population at $z \gg 3$ is similar to that of the U_{300}-dropout LBGs at $z \sim 3$, whose *observed* characteristics are, by now, reasonably well known even if their intrinsic properties, such as dust content, star-formation rate, mass, etc., are the subject of continued debate. In particular, we adopt the rest-frame UV luminosity function and UV spectral slope (i.e. intrinsic colour) distribution for LBGs at $\langle z \rangle \approx 3$ derived in Steidel *et al.* (1999), and use this to predict what should be seen in colour–colour diagrams *if* the same population were present at higher redshifts. We do this via Monte Carlo simulations, including realistic errors for the HDF WFPC2 + NICMOS photometry, comparing the number

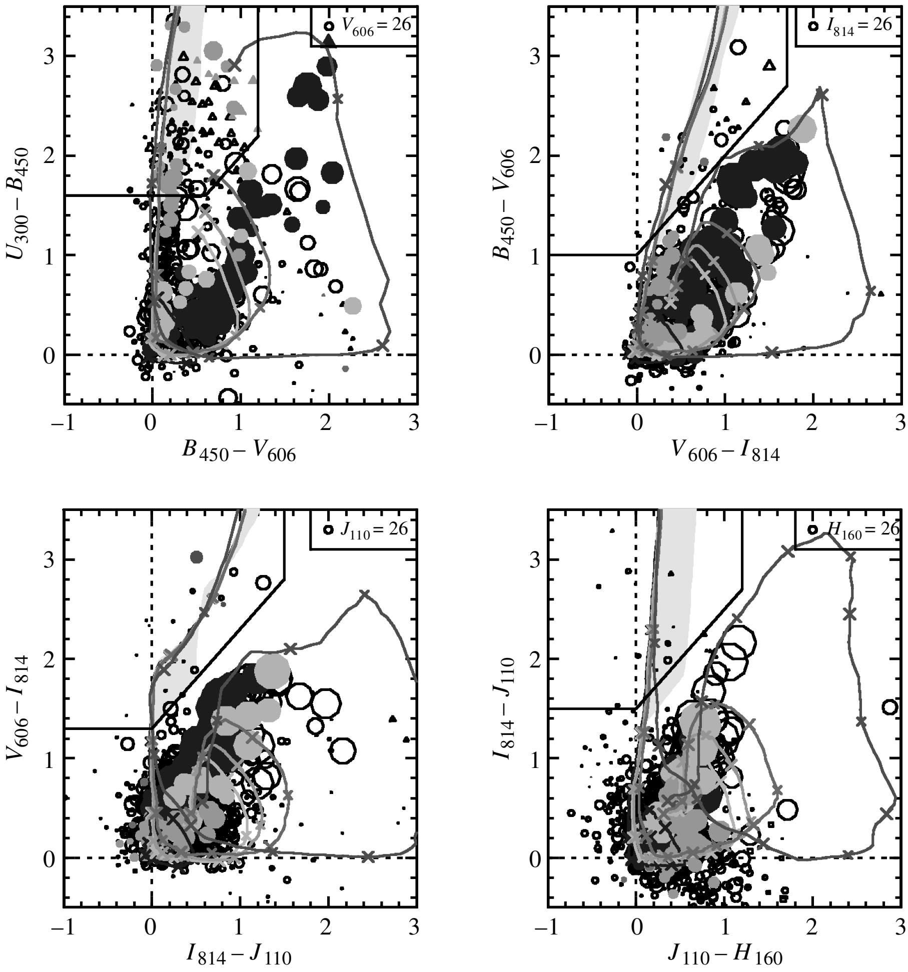

Figure 6. Two-colour diagrams for combinations of adjacent HDF WFPC2 + NICMOS filters. Symbol size scales with magnitude; known and suspected stars and a few bright galaxies have been excluded for clarity. Triangles mark 1σ lower colour limits; filled symbols indicate galaxies with spectroscopic redshifts. The lines show the nominal colour-versus-z tracks for various unevolving galaxy SEDs, and the shaded region indicates the approximate colour range expected for galaxies in redshift ranges appropriate to each colour pair (UBV: 2–3.5; BVI: 3.5–4.5; VIJ: 4.5–6; IJH: 6–8.5). The colour-selection boxes used for the comparison with Monte Carlo simulations are indicated.

of high-z objects that are predicted to fall in some specified colour–colour box with the actual number of similar objects found in the HDF catalogues.

Figure 6 shows a series of two-colour diagrams for the HDF, each using combinations of three adjacent bandpasses, from UBV (i.e. $z \sim 3$ selection) through IJH (i.e. $z \sim 7$). In each case, I define somewhat arbitrary selection boxes based on the expected location of high-redshift galaxies in colour–colour space (and also to avoid low-redshift contaminants), then count the galaxies in those boxes and compare this number with the 'no-evolution' (NE) model predictions (figure 7).

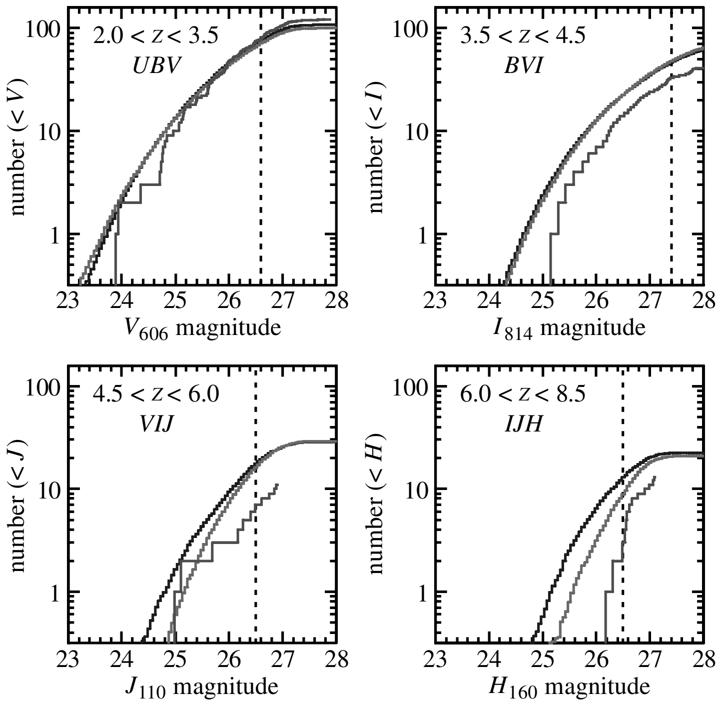

Figure 7. Cumulative number counts of objects satisfying the high-redshift colour criteria shown in figure 6. The irregular histograms are from the HDF data, and the 'smoother' histograms are predictions from the Monte Carlo simulations, which assume that the galaxy population at high redshift is like that observed at $z \approx 3$. Models were computed for two $\Lambda = 0$ cosmologies: $\Omega_{\mathrm{M}} = 1.0$ and 0.2 (the open cosmology is the lower model in the VIJ and IJH plots). The vertical dashed line indicates a rough 'confidence limit' in magnitude for each plot, below which the data should become significantly incomplete and/or contaminated by spurious sources.

The U_{300}-dropout counts agree well with the models by construction, since the input luminosity function is partly based on HDF data. The B_{450}-dropouts fall below the NE predictions. This is just the original Madau *et al*. (1996) result revisited: the HDF-north appears to have fewer galaxies at $z \sim 4$ than at $z \sim 3$. Steidel *et al*. (1999), who surveyed larger solid angles in several fields, suggest that the bright end of the $z \sim 4$ luminosity function (LF) is actually compatible with that at $z \sim 3$. The HDF may just be an anomaly, indicating the importance of field-to-field fluctuations, or perhaps the faint end slope of the LF (to which the HDF number counts are quite sensitive) evolves with redshift. For the V_{606}-dropouts, there are approximately seven candidates with $J_{110} < 26.5$ (including the two with spectroscopic confirmation), compared with a prediction of approximately 17. Careful inspection of their images and SEDs suggests that they are all very plausible $4.5 \lesssim z \lesssim 6$ candidates. There are *no* I_{814}-dropout candidates with $H_{160} < 26$, and only two with $H_{160} < 26.5$, one of which is clearly detected at B_{450} and V_{606} and, thus, is probably not at $z > 6$. The models predict 9–13 objects to this magnitude limit. Some of the fainter objects may be real $z > 6$ galaxies, but, on visual inspection, many are rather dubious, with very low S/N; only a few are persuasive to a sceptical eye. At $H_{160} > 26.5$ we are reaching or passing the useful depth limits of our NICMOS data for this purpose.

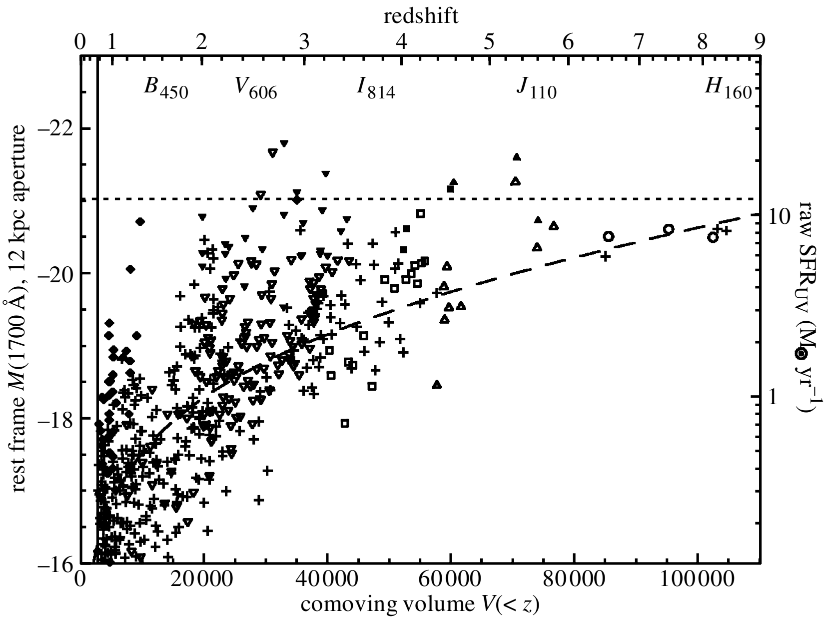

Figure 8. UV luminosity at λ_0 1700 Å versus comoving volume out to redshift z for galaxies with $H_{160} < 26.5$. A constant horizontal density of objects implies a constant space density. Fluxes are measured through $12h_{70}^{-1}$ kpc diameter metric apertures at all redshifts. The right-hand axis indicates the corresponding 'raw' star-formation rate derived from the UV luminosity without correction for dust, assuming a Salpeter IMF. The horizontal dotted line marks the luminosity of an L^* LBG at $z \approx 3$ (Steidel *et al.* 1999). The dashed curve indicates $m(\lambda_0 1700) = 26.5$ at the bandpass indicated by labels at the top. Objects with spectroscopic redshifts are indicated by filled symbols; photometric redshifts are used otherwise. Objects meeting two-colour criteria as U_{300}, B_{450}, V_{606} and I_{814} 'dropouts' are coded as ▿, □, △ and ○, respectively; all others are plotted with + and ♦.

This analysis is in qualitative agreement with one based on photometric redshift estimates. Figure 8 plots rest-frame 1700 Å luminosities of galaxies versus redshift (spectroscopic when available, photometric otherwise) for an HDF sample limited to $H_{160} < 26.5$. The photometric redshifts are generally in good agreement with the simple two-colour selection illustrated in figure 6. There are a few objects with $z_{\rm phot} \approx 3.5$ that 'fall in the gap' between the U_{300}- and B_{450}-dropout samples. At $z_{\rm phot} > 6$ there is only partial overlap between the I_{814}-dropout and photometric redshift samples, but this is understandable since most of the candidates are very faint with low-S/N photometry and poor photometric redshift constraints (i.e. relatively flat $z_{\rm phot}$ likelihood functions). The space density of the bright LBG candidates appears to thin at $z \gtrsim 4.5$, and at $z > 5.5$ there are no candidates with UV luminosities greater than the characteristic L^* at $z = 3$, despite abundant volume to house them if they were present with similar space densities.†

Ferguson (1998) and Lanzetta *et al.* (1999) have stressed the importance of cosmological surface-brightness dimming when characterizing the galaxy population at

† For an open universe, the higher $z_{\rm phot}$ candidates would be more luminous and the upper envelope to their UV luminosity would be nearly flat, but the space densities would be even more sparse compared with those at $2 < z < 3.5$.

$z > 3$. This can affect the likelihood of detecting high-redshift galaxies, as well as the fluxes measured with isophotally based photometry schemes. Lanzetta *et al*. (1999) show that the global rate of star formation occurring in the regions with the highest UV surface brightness rises steeply with redshift, and argue that far more UV light may be present in $z > 5$ galaxies at fainter, unmeasured isophotal thresholds. We may partly address this by measuring fluxes and luminosities non-isophotally, e.g. by using apertures scaled by image moments or with fixed metric sizes. The photometry in figure 8 uses 12 kpc metric apertures, and, thus, is insensitive to surface-brightness limits except as far as they affect galaxy detection in the first place: most faint object cataloguing packages use isophotal detection thresholds. We have examined this by taking WFPC2 images of $z \sim 2.5$ LBGs, artificially shifting them to higher redshifts, and re-inserting them into the NICMOS data to assess their detectability. Galaxies like the $L \gtrsim L^*$ LBGs at $z \sim 3$ should be detectable to at least $z \approx 7$ at the depth of our guest observer NICMOS images, and more easily in the HDF-south NICMOS field or the HDF-north GTO NICMOS image, each of which goes *ca.* 1 mag deeper than the dataset discussed here. However, a general census at such redshifts might indeed be woefully incomplete.

Overall, the HDF data disfavour the null hypothesis that galaxies like the bright LBGs at $2 < z < 4.5$ are present at $z \gg 5$ with similar space densities. The higher-redshift galaxies are apparently either fainter, more rare, have lower surface brightness, or some combination thereof. At any rate, they are certainly more difficult to detect and study, at least in abundance, even with the NICMOS.

6. An object at $z \gtrsim 12$?

Although the few I-dropout candidates in the HDF are very faint, paradoxically there is one comparatively bright 'J-dropout' object (shown in figure 9). Lanzetta *et al*. (1998) identified five possible sources in the KPNO K_s images of the HDF that were invisible in the WFPC2 data. Of these, four are undetected by the NICMOS. One, however, which we call HDFN-JD1, has a robust 1.6 μm detection ($H_{160} \approx 25.2$), but is at best only marginally ($S/N < 2$) detected at 1.1 μm and shorter wavelengths. This optical 'detection', if real, would be important, as it would probably exclude the most exotic hypothesis for this object, i.e. that it is a galaxy or QSO at $z \gtrsim 10$. It will be difficult, however, to obtain much deeper optical data than the existing HDF WFPC2 images to provide a stricter limit. The red $H_{160} - K_s$ colour suggests $z \approx 12.5$ under the high-redshift hypothesis, with the Lyα forest partly suppressing the H_{160} flux. We obtained an H-band spectrogram of HDFN-JD1 with a cryogenic spectrograph at the KPNO 4m, and, to our surprise, detected a moderately convincing emission line at 1.65 μm that could plausibly agree with Lyα at $z = 12.5$. The line did not reproduce, however, in a reobservation at higher dispersion (see Dickinson *et al*. (2000) for the spectra and further discussion).

If this is not a Lyman-break object, then it may be either heavily reddened and at arbitrary redshift (but most likely $z > 2$, given the colours), or, possibly, a maximally old elliptical galaxy at $3 < z < 4$ (see § 2). If it is really at $z \approx 12.5$, then it is either a galaxy whose unobscured star-formation rate (computed from the UV luminosity) is several hundred $M_{\odot}$ yr^{-1}, or an active galactic nucleus, perhaps one of the hypothesized population responsible for reionizing the Universe. If so, however, such objects are rare at $2 < z < 13$, with a space density several hundred times lower

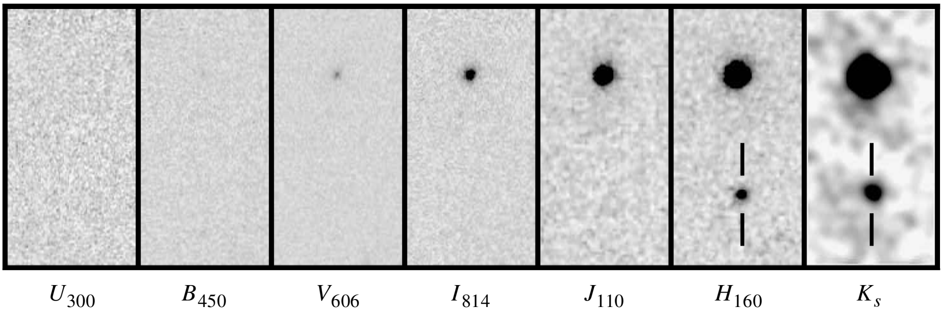

Figure 9. HST and Keck images of HDFN-JD1 at 0.3–2.16 μm. The field of view of each panel is 4 × 8 arcsec^2. HDFN-JD1 is identified by tick marks in the H_{160} and K_s panels. The Keck K_s image has been smoothed by a Gaussian with FWHM = 0.″38.

Table 1. *Properties of selected high-redshift galaxies and galaxy candidates*

(Assumes $\Omega_M = 0.3$, $\Omega_\Lambda = 0.7$, $h = 0.7$, and that SFR $= 1 M_\odot\ \mathrm{yr}^{-1}$ produces $L_\nu(1700\ \text{Å}) = 9 \times 10^{27}\ \mathrm{erg\ s^{-1}\ Hz^{-1}}$. Magnitudes are on the AB scale.)

name	z	m (UV at *ca.* λ_0 1700 Å)	M (UV at *ca.* λ_0 1700 Å)	L/L^* (UV at *ca.* λ_0 1700 Å)	'raw' SFR ($M_\odot\ \mathrm{yr}^{-1}$)	reference
L^* LBG	3.04	24.5	−21.1	≡1	12.8	Steidel *et al.* (1999)
CDFa-G1	4.82	23.6	−22.8	4.7	60	Steidel *et al.* (1999)
RD1	5.34	25.5:	−21.0:	0.9:	12:	Dey *et al.* (1998)
HDF 3-951	5.33	25.0	−21.5	1.5	19.6	Spinrad *et al.* (1998)
HDF 4-473	5.60	26.0	−20.6	0.66	8.5	Weymann *et al.* (1998)
HCM1	5.74	25.5:	−21.1:	1.1:	13.5	Hu *et al.* (1999)
A	6.68	23.9:	−23:	5.8:	74:	Chen *et al.* (1999)
HDFN-JD1	12.5 ??	23.9	−23.9	13.7	175	Dickinson *et al.* (2000)

than that of present-day L^* galaxies, and it is unlikely that most of today's galaxies began their life in such a way.

Table 1 compares the UV luminosities of some confirmed and candidate galaxies at $z > 4$ with that of an L^* LBG at $z = 3$. In some cases, IR data needed to measure fluxes at rest frame 1700 Å are not available, and estimates based on published photometric or spectroscopic fluxes redward of Lyα have been used instead.† 'Raw' star-formation rates are computed from the UV luminosities assuming a Salpeter IMF and no dust obscuration.

CDFa-G1 at $z = 4.815$ is the most-luminous LBG yet identified (among both U_n- and G-dropouts) in our large, ground-based survey. The spectroscopically verified $5 < z < 6$ galaxies have luminosities that are mostly fairly typical of $z \approx 3$ LBGs, ranging from 0.66 to $1.5L^*$. The $z = 5.74$ object from Hu *et al.* (1999) has been described as 'extremely luminous', but is actually quite typical for $z \approx 3$–4 LBGs, and somewhat fainter than HDF 3-951 at $z = 5.33$. Chen *et al.* (1999) have identified a candidate galaxy at $z = 6.68$ from Space Telescope Imaging Spectrograph (STIS)

† $L_\nu(1700\ \text{Å})$ estimates for RD1 are derived in part from a J-band measurement by Armus *et al.* (1998). For HDF 3-951 and 4-473 we use our own NICMOS J_{110} photometry.

slitless spectra. The available photometry is limited, but based on the spectral continuum flux-density estimate, this object appears to be significantly more luminous than other known LBGs at $2 < z < 6$, or than any $0 < z < 10$ candidates from the HDF/NICMOS sample. This is a remarkable result, if true, since the solid angle covered by the STIS field is less than 1 arcmin^2. On the other hand, if the J-dropout object HDFN-JD1 was really at $z = 12.5$, it would be more luminous still, nearly three times brighter than CDFa-G1 at $z = 4.82$, with a 'raw' UV SFR $= 175 M_\odot$ yr^{-1}.

7. Discussion

Overall, the HDF/NICMOS data demonstrate both the promise and the challenges that lie ahead for finding and studying the 'first' galaxies. The rest-frame optical view of LBGs presented in §§ 2 and 3 strongly suggests that the galaxy population at $2 < z < 3$ had not yet achieved maturity. The giant Hubble sequence spirals and ellipticals that dominate the high-mass end of the galaxy population today are not seen at $z > 2$. In a sample of HDF galaxies selected in the NIR, nearly all galaxies with spectroscopic or plausible photometric redshifts $2 < z < 3.5$ are evidently forming stars quite rapidly and can also be identified via their emitted-frame UV light. The evidence from the SCUBA shows that there are occasional 'monsters' whose obscured star formation may be quite important to the global emissive energy budget from galaxies. The identification of these objects, relatively rare by number, remains an important dilemma.

Broadband colour selection has been the most successful means for identifying high-redshift galaxies, but we seem to be pushing the limits of what can be accomplished at $z > 6$ with present-day capabilities. The NICMOS HDF images are the deepest NIR data now available, and they do include plausible candidates for galaxies at $6 < z < 9$, but they are relatively few, and most are quite probably too faint for spectroscopic confirmation. We probably should not expect to find galaxies much *brighter* than these candidates unless some of the 'first' galaxies were significantly more luminous than the boring, old, 'later' galaxies that we have now surveyed extensively at $z \approx 3$. This is not impossible of course: the Chen *et al*. (1999) object and HDFN-JD1 are both possible (but unconfirmed) $z > 6$ candidates more luminous than any normal LBG at $z < 5$. Perhaps, indeed, there are very luminous, relatively unobscured proto-galaxies out there waiting to be found, a hope that was once quite widespread, but which seems to have gradually faded in the modern era of 25th magnitude LBGs and optically invisible SCUBA sources. Perhaps it will still make a comeback.

These few rather speculative candidates aside, the evidence from the HDF alone would suggest that the population of UV-bright LBGs may be thinning out at $z > 5$, at least for objects comparable with those at the bright end of the $z \approx 3$ luminosity function. It should be remembered, however, that this was also the conclusion reached by Madau *et al*. (1996) at $z > 3.5$, a result that has since been challenged by larger surveys with extensive spectroscopy. It is undoubtedly dangerous to draw conclusions too strongly from one 5 arcmin^2 field. However, extending this work to larger areas and more sightlines will be an expensive effort. Surface-brightness dimming and limited solid-angle coverage may limit our ability to see much more with the NICMOS (assuming that it is successfully revived in 2001), and ground-based NIR imaging may never go deep enough to detect any but the most luminous objects at $z > 5$. Wider fields imaged with the HST WFC3 NIR channel (coming circa 2004) may offer the best survey opportunity until NGST, but a substantial investment of observing time will be needed to survey adequate solid angles to sufficient depth.

Alternatively, we may turn to other observing strategies, e.g. by taking advantage of gravitational lensing from foreground galaxy clusters to boost very distant objects to detectable magnitudes. Narrow-band and blind multislit emission line searches are being carried out through airglow windows (e.g. at λ9150 Å, corresponding to $z \approx 6.5$; cf. Crampton & Lilly (1999) and Stockton (1999)). Or perhaps concerted efforts to identify SCUBA sources will indeed turn up objects at $z \gg 5$, where the advantage of the negative SMM k-correction is enormous.

These data are offering a first glimpse into the so-called 'dark ages', and giving hope that there may be luminous things there to find and study. In some sense, we may not know that we have found the first galaxies until we can find no more beyond them. Holding to that standard will ensure that a more challenging (and, hence, more rewarding) threshold of proof always lies ahead.

I thank my HDF/NICMOS collaborators for their contributions and for permission to show results in advance of publication, particularly Casey Papovich, Tamas Budavári, Jean-Marc Deltorn, Chris Hanley and Harry Ferguson. I also thank Chuck Steidel, Max Pettini, Mauro Giavalisco, Kurt Adelberger and Alice Shapely for their long-standing and highly valued collaboration. I am grateful to The Royal Society for inviting me to this Meeting and for supporting my travel and accommodation, and to the editors of this issue for their patience. This work was supported by NASA grant GO-07817.01-96A.

References

Armus, L., Matthews, K., Neugebauer, G. & Soifer, B. T. 1998 *Astrophys. J.* **506**, L89.

Barger, A. J., Cowie, L. L., Trentham, N., Fulton, E., Hu, E. M., Songaila, A. & Hall, D. 1999 *Astr. J.* **117**, 102.

Budavári, T., Szalay, A. S., Connolly, A. J., Csabai, I. & Dickinson, M. 2000 *Astr. J.* (In the press.)

Bunker, A. J. 1999 In *Photometric redshifts and the detection of high-redshift galaxies* (ed. R. Weymann, L. Storrie-Lombardi, M. Sawicki & R. Brunner), p. 317. San Francisco: Astronomical Society of the Pacific.

Calzetti, D. 1997 In *The ultraviolet Universe at low and high redshift* (ed. W. H. Waller *et al.*), p. 403. New York: American Institute of Physics.

Chen, H.-W., Lanzetta, K. M. & Pascarelle, S. 1999 *Nature* **398**, 586.

Crampton, D. & Lilly, S. 1999 In *Photometric redshifts and the detection of high-redshift galaxies* (ed. R. Weymann, L. Storrie-Lombardi, M. Sawicki & R. Brunner), p. 229. San Francisco: Astronomical Society of the Pacific.

Dey, A., Spinrad, H., Stern, D., Graham, J. R. & Chaffee, F. H. 1998 *Astrophys. J.* **498**, L93.

Dickinson, M. 1998 In *The Hubble deep field* (ed. M. Livio, S. M. Fall & P. Madau), p. 219. Cambridge University Press.

Dickinson, M. 2000 In *Proc. XIXth Moriond Astrophysics Mtg* (ed. F. Hammer, T. X. Thuan, V. Cayatte, B. Guiderdoni & J. Tranh Than Van), p. 257. Editions Frontières. (In the press.)

Dickinson, M. *et al.* 2000 *Astrophys. J.* **531**, 624.

Ferguson, H. C. 1998 In *The Hubble deep field* (ed. M. Livio, S. M. Fall & P. Madau), p. 181. Cambridge University Press.

Fernández-Soto, A., Lanzetta, K. M. & Yahil, A. 1999 *Astrophys. J.* **513**, 34.

Giavalisco, M., Steidel, C. C. & Macchetto, D. 1996 *Astrophys. J.* **470**, 189.

Hogg, D. W., Neugebauer, G., Armus, L., Matthews, K., Pahre, M. A., Soifer, B. T. & Weinberger, A. J. 1997 *Astr. J.* **113**, 2338.

Hu, E. M., McMahon, R. G. & Cowie, L. L. 1999 *Astrophys. J.* **522**, L9.

Hughes, D. *et al.* 1998 *Nature* **394**, 241.

Kinney, A. L., Calzetti, D., Bohlin, R. C., McQuade, K., Storchi-Bergmann, T. & Schmitt, H. R. 1996 *Astrophys. J.* **467**, 38.

Lanzetta, K. M., Yahil, A. & Fernández-Soto, A. 1996 *Nature* **381**, 759.

Lanzetta, K. M., Yahil, A. & Fernández-Soto, A. 1998 *Astr. J.* **116**, 1066.

Lanzetta, K. M., Chen, H.-W., Fernández-Soto, A., Pascarelle, S., Puetter, R., Yahata, N. & Yahil, A. 1999 In *Photometric redshifts and the detection of high-redshift galaxies* (ed. R. Weymann, L. Storrie-Lombardi, M. Sawicki & R. Brunner), p. 223. San Francisco: Astronomical Society of the Pacific.

Lilly, S. *et al.* 1998 *Astrophys. J.* **500**, 75.

Lowenthal, J. D. *et al.* 1997 *Astrophys. J.* **481**, 673.

Madau, P., Ferguson, H. C., Dickinson, M., Giavalisco, M., Steidel, C. C. & Fruchter, A. S. 1996 *Mon. Not. R. Astr. Soc.* **283**, 1388.

Meurer, G. R., Heckman, T. M., Lehnert, M. D., Leitherer, C. & Lowenthal, J. 1997 *Astr. J.* **114**, 54.

Meurer, G. R., Heckman, T. M. & Calzetti, D. 1999 *Astrophys. J.* **521**, 64.

Papovich, C. *et al.* 2000 (In preparation.)

Pettini, M., Kellogg, M., Steidel, C. C., Dickinson, M., Adelberger, K. L. & Giavalisco, M. 1998 *Astrophys. J.* **508**, 539.

Richards, E. A., Kellerman, K. I., Fomalont, E. B., Windhorst, R. A. & Partridge, R. B. 1998 *Astr. J.* **116**, 1039.

Sawicki, M. & Yee, H. K. C. 1998 *Astr. J.* **115**, 1329.

Simard, L. *et al.* 1999 *Astrophys. J.* **519**, 563.

Spinrad, H., Stern, D., Bunker, A., Dey, A., Lanzetta, K. M., Yahil, A., Pascarelle, S. & Fernández-Soto, A. 1998 *Astr. J.* **116**, 2617.

Stanford, S. A. *et al.* 2000 (In preparation.)

Steidel, C. C., Giavalisco, M., Pettini, M., Dickinson, M. & Adelberger, K. L. 1996 *Astrophys. J.* **462**, L17.

Steidel, C. C., Adelberger, K. L., Giavalisco, M., Dickinson, M. & Pettini, M. 1999 *Astrophys. J.* **519**, 1.

Stockton, A. 1999 In *Toward a new millenium in galaxy morphology* (ed. D. L. Block, I. Puerari, A. Stockton & D. Ferreira). Dordrecht: Kluwer.

Thompson, R. I., Storrie-Lombardi, L. J., Weymann, R. J., Rieke, M., Schneider, G., Stobie, E. & Lytle, D. 1999 *Astr. J.* **117**, 17.

Weymann, R. J., Stern, D., Bunker, A., Spinrad, H., Chaffee, F. H., Thompson, R. I. & Storrie-Lombardi, L. J. 1998 *Astrophys. J.* **505**, L95.